Contents lists available at ScienceDirect

Heliyon

Spatial distribution of aerosols burden and evaluation of changes in aerosol optical depth using multi-approach observations in tropical region

Najib Yusuf [a,b,c,*], Rabia S. Sa'id [c]

[a] NASRDA'S Centre for Atmospheric Research (CAR), Anyigba, Kogi State, Nigeria
[b] National Centre for Atmospheric Research (NCAR), Boulder, CO, USA
[c] Department of Physics, Bayero University Kano, Nigeria

ARTICLE INFO

ABSTRACT

Understanding of Aerosol optical depth (AOD) parameter is important for air quality assessment. This study aims to evaluate and validate AOD measurements from combine datasets to improve air quality for a period 2005–2020 using Aerosol Robotic Network (AERONET) at Ilorin site (8.320° N, 4.340° E) in Nigeria. AOD outputs from Community Atmosphere Model Version 6 with chemistry (CAM6-chem) at 1° horizontal resolution and Modern-Era Retrospective analysis for Research and Applications (MERRA-2) are investigated in addition to validation of two satellites AOD retrievals: Moderate Resolution Imaging Spectroradiometer (MODIS) and Multi-angle Imaging Spectroradiometer (MISR). Result of spatial distribution of AOD shows high values > 1 in the North and Western Sahara compared to Central Africa. Desert dust shows largest contribution in the North and Western Africa that is up to 2 magnitude larger than other aerosol types. Primary organic matter (POM) and secondary organic aerosols (SOAs) both presents high burdens with later been dominant at around 10° band, and black carbon (BC) largest burden ($2.6 \times 10 - ^5 kgm - ^2$) is seen in the model from oil and gas exploration site in Nigeria. Inter-comparison of MERRA/MISR/MODIS and AERONET AOD using linear correlation of the seasonal dependence demonstrated high correlation ($r = 0.864 - 0.973$) subjected to Root Mean Square Error (RMSE = 0.069 − 0.211), suggesting good agreement between the datasets. When compared to seasonal mean maximum AERONET AOD value of 0.978 MERRA is ~5%, MISR ~28% and MODIS ~29% lower with stronger correlations observed in the wet and pre-harmattan seasons. Similarly, MODEL AOD at 550 nm and dust burden were found to be ~34% and ~67% lower in context to AERONET AOD annual mean value of 0.627. Positive relationships that indicate an upward slope exist between all the computed datasets with moderate value of AERONET/CAM-chem spearman partial correlation, and MERRA/MODIS and MODIS/MISR showing strong and significant relationship with p-value less than 0.05. Low variance is observed with all measurements except in MERRA.

* Corresponding author. Centre for Atmospheric Research (CAR), National Space Research and Development Agency (NASRDA). P. O. Box 380, Prince Abubakar Audu University Campus. Kogi State, Anyigba, Nigeria.
E-mail address: najiby@carnasrda.com (N. Yusuf).

1. Introduction

Exposure to outdoor air pollution is estimated to have caused approximately 7 million premature death per annum (WHO, 2016, 2018a), unfortunately, 99% of the world's population lives in places where the WHO air quality guiding principles levels are not met. Thus, air quality at present is the largest environmental hazard that influence human health. African countries, such as Nigeria is categorized amid the leading countries with poor air quality [1]. Africa is a unique region because it is among the global largest sources of emitted pollutants resulted from rapid population growth, urbanization and agriculture practices United Nations Population Division, (2014), and limited legislation measures among others, hence, African air pollution present a demanding solution, and this sparse environment has not been fully investigated [2,3].

The composition of aerosol particles in the atmosphere over Africa exhibits a unique complex mixture due to different emission sources comprises of both natural and anthropogenic particles [4–6]. This mixture contributes to different pollutants in the atmosphere over the region. Anthropogenic emissions of both primary particles and precursor gases contribute substantially to the total aerosols burden (Giglio et al., 2013; Magi et al., 2012; [7].

Previous campaigns from the African monsoon multi-disciplinary analyses [8–11] and work using a bottom-up method predicts an increase in BC, CO, NOX, SO$_2$ and non-methane hydrocarbon emissions over Africa by 2030 if no regulations are implemented in the region (Liouse et al., 2014). Other field campaigns includes the dynamics aerosol chemistry cloud interactions have presents air quality predicaments in West Africa [12]. The development of Africa specific emissions inventory diffuse inefficient combustion emissions inventory by Marais and Wiedinmyer [13], and other efforts from (Assamoi & Liousse, 2010 [14]; also contribute significantly in understanding emissions in the region. Additionally, previous modeling studies found that exposure to outdoor air pollution has led to 176,000 deaths and 626,000 disability adjusted life years in sub-Saharan Africa [3], and it is expected that these numbers are much higher in reality due to the limited data emanating from the region. Air quality models, such as CHIMERE [15] or PMCAMx [16] allow the simulation of past, present, and future air pollution.

Residential and biomass emissions from agricultural activities are the main drivers of anthropogenic emissions in Africa contributing about 14, 000 premature deaths linked to ambient particulate matter in 2013 [4,10,17,18]. Additionally important is natural sources including desert dust aerosols from the Sahara and local dust. However, anthropogenic emissions from industrial and transportation sectors may likely surpass residential sector as the key contributors to poor air quality by 2030 in the region [14].

Exposure to Black Carbon (BC) due to biomass emissions that is a strong component of particulate matter accounts for approximately 3.7 million premature deaths per year worldwide [19,20], with solid fuel use contributing to approximately 0.5 million [21]. Lacey and Henze [22], have also shown that cookstoves and other residential sources such as firewood and charcoal are responsible for about 20% of the current BC emission in the region. The current global hike in gas price will force many communities to resolve to the use of charcoal and fire-wood for domestic cooking and this will eventually leads to more emissions particularly in Africa if no stringent measures are taken.

The impact of these emitted pollutants on air quality over West Africa is uncertain [14] due to primarily limited air quality monitoring networks [2]. This shortcoming leaves satellite observations and modeling as the only alternative to studying air quality and AOD [23]; Kahn et al., 2018 [24]: in the region. To achieve the precision satellite retrievals are often validated with surface observation.

The main focus of this paper is to use ground-based AERONET observation to evaluate the CAM6-chem and MERRA 2 AOD outputs and also to validate AOD from two radiospectrometers towards improving air quality in West Africa. Aside this, the paper also discussed six (6) key aerosols types in air quality monitoring: desert dust aerosol, primary organic matter, secondary organic aerosols, black carbon, sulfate aerosols and seasalt.

Section 2 presents the data sources and methods. Section 3 presents the results and discussed the model AOD and aerosols burden over Africa and also comparison of different datasets including seasonal, interannual variabilities and anomaly. Finally, Sect. 4 presents the conclusion.

2. Data source and methods

2.1. CAM-chem

Community atmosphere model with chemistry CAM6-chem is the atmosphere component of the Community earth system model (CESM). We implement CAM6-chem in CESM2.0 configuration to estimate changes in atmospheric composition in Africa by simulating the amount of various aerosol types in the atmosphere in the region. The meteorological data and the initial boundary condition used were both from an assimilated meteorology from MERRA-2 reanalysis product [25]. For emissions, the community emissions data system (CEDS) for coupled model inter-comparison project phase 6 (CMIP6) inventory Hoesly et al. (2018) was used in this configuration. The model version (CESM2.0) is based on the earlier version as described in Hurrell, Holland, & Gent, [26]. The physics configuration is an updated CAM6 physics as described in Ref. [27]. The model is coupled to the new community land model version 5.0 (CLM5.0). The chemistry model includes comprehensive tropospheric and stratospheric chemistry, as described in Ref. [28]; with updates as described and evaluated in Ref. [29]. The aerosol scheme used in this model configuration is the modal aerosol model (MAM3), which was coupled to the physical model to include both aerosol direct and indirect effects, as described in Refs. [30–32]. Further, a new volatility bin scheme is implemented to improve the description of organic aerosols in the model following the approach by Ref. [33]; as described and evaluated in Ref. [34]. The atmospheric model runs on a horizontal resolution of 0.9 × 1.25° and on 32 vertical layers from the surface up to about 3 hPa, using observed sea-surface temperatures. Applying the model in this geolocation is

important due to the fact that this is among the pioneer research with which the model is applied in Nigeria's terrain. CESM Project, http://www.cesm.ucar.edu/models/cesm2/atmosphere/.

2.2. Aerosols burden

Spatial distributions of multi-year (2005–2014) mean of various aerosol burdens and MODEL AOD at wavelength 550 nm were analyzed. Burden of aerosols is the quantity or concentrations often in kilogram of a specific aerosol specie compared to the total aerosol loading in the atmosphere of the study area. We deduce the burden of each aerosol species from the total concentrations of aerosol load estimated in the model over Africa and average each species to produce multi-year average for a period of 2005–2014 (based on our interest) over Africa. These computed averages were used to produce the spatial distributions of various aerosols species under study: desert dust, primary organic matter, secondary organic aerosols, black carbon, sulfate and seasalt. Additionally, we combined both concentrations in the day and night to have a total concentrations of each specie in the region.

2.3. Aeronet AOD

AERONET is a network of ground-based sun/sky photometers taking real-time ground-based remote sensing measurements of aerosols optical properties. The data is validated against other data archives and the network is known for its standardization of instruments, calibration, processing and distribution [35,36]. Aerosol optical depth data are computed at three different data quality levels: Level 1.0 (unscreened), Level 1.5 (cloud-screened), and Level 2.0 (cloud screened and quality-assured). Version 2 Level 2.0 quality-assured and cloud screened data with a minimal uncertainty was utilized in this region (see Ref. [37]. The accuracy and precision in the measurement is scientifically validated and data retrieval and data quality control are reasonable [38,39]. AERONET data can be accessed https://aeronet.gsfc.nasa.gov/new_web/data.html.

Here, AERONET remote sensing ground-based measurements of aerosol optical depth at wavelength 550 nm was computed from 440 nm to 675 nm AERONET AOD retrievals using Ångström exponent equation as described in Ref. [37] and applied it to evaluate the corresponding CAM6-chem AOD (hereafter refers as MODEL AOD) and MERRA AOD as well as validating satellites AOD retrievals and at Ilorin AERONET site in Nigeria. For the model we compared the multi-year (decadal) mean MODEL AOD, MODEL dust to the corresponding multi-year mean AERONET AOD at 550 nm wavelength using temporal distribution for a period 2005–2014. This multi-year mean from AERONET AOD observations are compared with the corresponding calculated multi-year mean from the MODEL AOD output as well as model dust. We employed statistical approach: linear correlation coefficient r, R-square, standard deviation, root mean square error, mean absolute error and percentage correlation to investigate the relations between different AOD measurements at Ilorin site in Nigeria. Similarly, comparison between the two spectroradiometers MODIS (2005–2020)/MISR (2005–2017) AODs and MERRA (2005–2020) AOD against the sunphotometer AERONET (2005–2020) AOD are carried out seasonally. However, correlation coefficient can only give an overall relation between the different measurements of AOD without presenting the seasonal dependence. Thus, AODs are computed seasonally by categorizing Nigeria into Four seasons DJF (as Harmattan), MAM (as pre-monsoon), JJA (as monsoon) and SON (as post–monsoon) in order to understand and achieve the seasonal dependency. Percentage of similarities are analyzed. Further, interannual variability and anomaly are calculated to establish the optical depth changes and bias in relation to surface AERONET AOD retrievals. Descriptive statistic functions of partial correlations with 2-tailed significance were employed to investigate the relationship between the MODEL and satellite's observed AODs and AERONET observation.

2.4. Satellites AOD retrievals

The connection of aerosols to climate and air quality has been achieved through data retrievals from satellites due to reasonable and continuous observation over large spatial coverage. This study utilizes AOD data from two spectroradiometers MODIS and MISR aboard American Aura satellite that is well known for providing aerosols product including optical properties of aerosols for climate and air quality studies (J.-F. [40]; van Donkelaar et al., 2016; Boucher et al., 2013). Satellites retrievals are accessed from NASA's Earth data Giovanni v 4.35 archive.

(a) Moderate Resolution Imaging Spectroradiometer (MODIS) has a wide spectral channels 36 to be precise and 12-bit radiometric resolutions ranges from visible to thermal infrared band with broad band shooting coverage of 2330 km at least once in a day [41]. MODIS has two components: Aqua crosses the Equator at 13:30 local time (LT) and its daylight measurements is carried out on the ascending part of its orbit and Terra crosses the local Equator at around 10:30 LT in a daytime-descending orbit (J.-F [40,42]. This gives MODIS the ability to provide aerosols product with uncertainty of ±0.05 ($\pm0.15 \times$ AOD) over land and ±0.03 ($\pm0.05 \times$ AOD) over the ocean, on daily scale covering both the land and bright surface such as desert as in Deep blue (DB) [43] and over the ocean and vegetation coupled with dark patches in the case of Dark target (DT) algorithm [44]. This coupling between the two algorithms especially in locations where there are very limited ground based stations, such as our study area, will provide a more precise and advance information in the current understanding of aerosols optical depth.

Level 3 gridded daily as well as monthly AODs product of MODIS has demonstrated to fit the AERONET observations for example in Refs. [45,46]. Also, a time interval of the satellite transect of ±30 min is ideal for comparison J.-F [40]. but considering the small area for the comparison of our interest [47,48], suggested that the gap could be more understood by statistical approach rather than physics. Based on this recommendation, we apply statistic to achieve our comparison goals as explained in subsection 2.3. Further, we
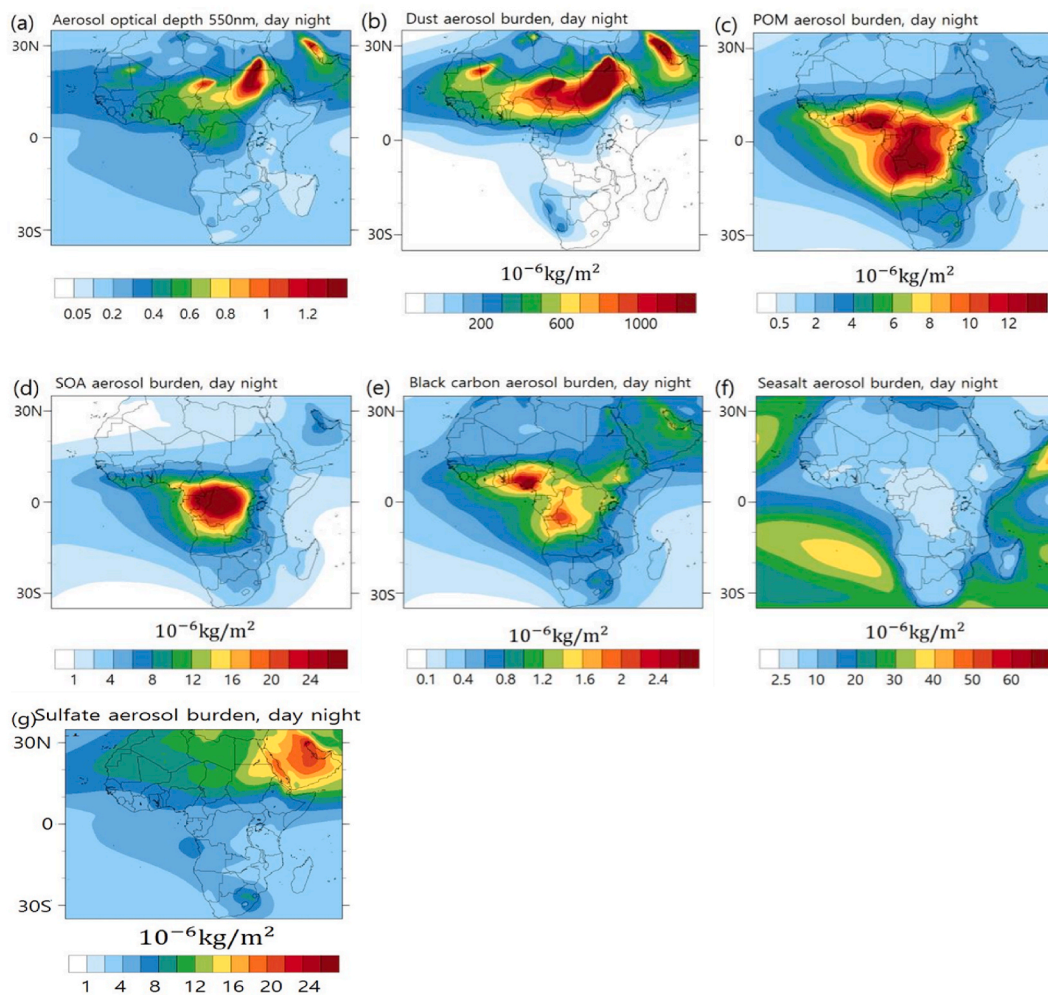
Fig. 1. CAM6-chem aerosols burden spatial distributions of multi-year (2005–2014 average; (a) model AOD (b) dust (c) POM (d) SOA € BC (g) seasalt and (f) sulfate.

combined the two files with common geolocation to reduce the uncertainty of both Aqua and Terra AOD retrievals and obtained the average to give a more competitive and comprehensive dataset for the comparison as well as seasonal dependence analysis of AOD over Ilorin AERONET site in Nigeria. This approach will yield a more coherent comparison with AERONET AOD as the Ilorin AERONET site falls in the tropical savanna climate, Köppen climate classification Aw with two distinct seasons [49,50].

(b) The Multi-angle Imaging SpectroRadiometer (MISR), has greater advantage over other satellites because of its shooting system that enables MISR to receive the longwave radiation in specifically nine various directions (nadir, 26.1, 45.6, 60.0 and 70.5° for backward as well as forward viewing using 9 different cameras, the arrangement of 14 bit push brooms cameras enable MISR to capture the entire planet in four spectral bands at each angle 446 ± 21, 558 ± 15, 672 ± 11 and 866 ± 20 nm in 7 min with medium and low space resolution (from 275 to 1100 m). Swath constitutes ~400 km width [51]. The MISR data AOD uncertainty is $0.05 \pm 0.2 \times$ AODAERONET [52].These advantages the MISR has over other remote sensing observations made the use of it in our quest to investigate AOD changes important and inevitable.

(c) Other important factor to consider in this comparison of AOD from the two spectroradiometers with surface sunphotometer observation is the meteorological influence and cloud reflection and the fact that most satellites are coarser in nature, these may induce some bias in the AOD retrievals as such we employ AOD from the Modern-Era Retrospective Analysis for Research, version 2 (MERRA-2) (Gelaro et al., 2017). MERRA-2 has an enhanced meteorological observing system as described in Refs. [53–55]. The combined data from models, satellite retrievals and surface observations used in MERRA-2 modeling may accord a technical and more precise approach in the representation of aerosol optical depth.
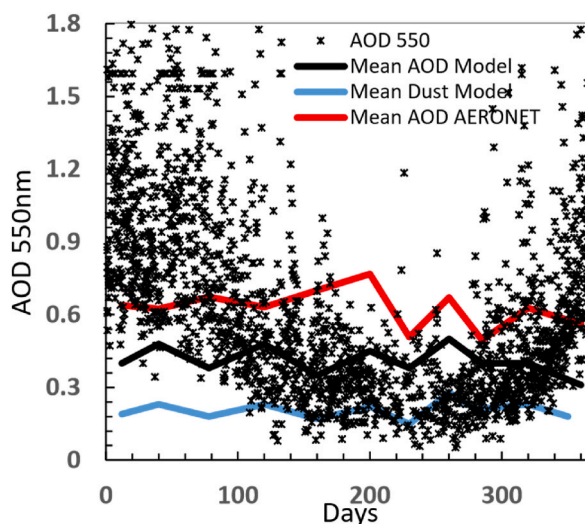
Fig. 2. Comparison of multi-year mean MODEL AOD (black line), AERONET AOD (red line) at 550 nm and model dust (blue line), AERONET AOD daily distribution (stars) for a period 2004_2015 at Ilorin AERONET site in Nigeria.

3. Results and discussion

3.1. Model AOD and aerosol burdens in Africa

Multi-year averaged MODEL AOD varies with latitude and the lowest values of 0.05–0.2 were seen in southern Africa low latitude and east of equatorial regions (Fig. 1a). High aerosol loading with mean MODEL AOD = 0.6 is found around equatorial region of west and central Africa and maximum value of MODEL AOD >1.2 in the north eastern part and low latitude north African region. Different regions have different aerosol compositions due to aerosol various sources. The high optical depth seen in the NE region is associated with the northern Sahara dust (Fig. 1a).

Fig. 1b shows multi-year averaged dust aerosol burden over the continent. The dust burden is by far the largest contributor of aerosol mass, with up to 2 magnitude larger than the other aerosol types (for example SOA) in the region. The dust aerosol highest burden estimated in the model ranges from $1.1 \times 10^{-3} \, kgm^{-2} - 1.2 \times 10^{-3} \, kgm^{-2}$ and are well pronounce in Niger republic, Chad, Sudan, Egypt and Mauritania. This is attributed to the nation's proximity to desert and the impact of easterlies that transport Saharan dust to the western Africa in addition to dust originating from Western Sahara.

Over Nigeria dust burden ranges from $4.0 \times 10^{-4} \, kgm^{-2} - 9.0 \times 10^{-4} \, kgm^{-2}$ from the south to far north near Bodélé depression. However, the southern African region has a comparatively low dust aerosol influence.

The high amount of dust aerosol seen in Nigeria from the model agrees to the percentage (76%) of coarse dust aerosol dominance as established based on particle size and volume size distribution from remote sensing ground-based AERONET measurement at Ilorin site in Nigeria [37]. The model estimates dust aerosol burden and the spatial distribution of dust in Nigeria as well as West Africa reasonably well.

Dust aerosols dominance is both seen in Nigeria from the model and AERONET observation as referenced. The knowledge of dust aerosol burden over the region is important because mineral desert dust is next to biomass emissions as the main driver of pollutants and is a strong component of particulate matter of aerodynamic diameter 2.5 (PM$_{2.5}$), as such, is second to fine particle aerosols as the contributor to mortality rate in African [4].

Primary organic matter (POM) results mainly from biogenic and biomass emissions generated both naturally and anthropogenically [56]. POM is dominant with high values of $1.2 \times 10^{-5} \, kgm^{-2} - 1.4 \times 10^{-5} \, kgm^{-2}$ at the equatorial low latitude regions (15° N − 15° S) (Fig. 1c). The maximum POM burden of $1.4 \times 10^{-5} \, kgm^{-2}$ is seen in DR Congo, Angola and Nigeria.

Similarly, Fig. 1d presents multi-year averaged of the secondary organic aerosols (SOAs) burden. SOAs produced from forests are dominant at around 10° band in central Africa low latitude region (Fig. 1d). Large values of SOAs are seen over the largest contiguous Congo forest, which is the second largest tropical rainforest globally, and covers a significant portion of Cameroon, Central African Republic, democratic republic of Congo, Equatorial Guinea and Gabon. Thus, biogenic emissions are likely the cause of high burden SOA in the central African region. Both POM and SOA burdens show substantial concentrations in the years of study (Fig. 1c and d). Moreover, POM is more disperse over Africa compared to SOA that has a twice larger burden with maximum concentration of $2.8 \times 10^{-5} \, kgm^{-2}$. However, North African region show relatively low POM and SOA burdens.

In Fig. 1e and f, multi-year average BC and seasalt spatial distributions in Africa are presented. Nigeria shows largest BC burden of $2.8 \times 10^{-6} \, kgm^{-2}$ in Africa (Fig. 2e). With high burden from the southern part at the epicenter of the oil and gas exploration states (Port Harcourt, Bayelsa, Delta etc.). Though, the southern part of Nigeria is a rainforest climate region, where agricultural activities result in large burning of biomass emissions that contribute significantly to the release of BC into the atmosphere, emissions from gas

Table 1

Descriptive statistics showing seasonal mean and percentage decrease, standard deviation, maximum, minimum, RMSE, MAE and *r* of MODEL AOD (550 nm), MODEL dust and AERONET.

	MODEL AOD 550 nm	MODEL dust	AERONET AOD 550 nm
Decadal Mean	0.422	0.209	0.634
Percentage decrease	33.0	67.0	100.0
Standard deviation	0.051	0.037	0.082
Maximum	0.501	0.280	0.767
Minimum	0.350	0.150	0.495
	AERONET AOD & MODEL AOD	AERONET AOD vs. MODEL Dust	MODEL AOD vs. MODEL Dust
r	0.317	0.307	0.812
RMSE	0.229	0.427	0.208
MAE	0.215	0.421	0.205

flaring especially in the Niger-delta oil and gas exploration contributes significantly to the release of anthropogenic VOCs and BC into the atmosphere. Thus, the likely cause of high BC burden in the region. BC is a strong component of $PM_{2.5}$, the presence of large quantity of BC in the atmosphere results in poor air quality that has deteriorating effect on health, for example modeling results have shown that approximately 273,000 premature mortality for adults greater than 30 years old and infants less than 5 years old are caused by outdoor $PM_{2.5}$ and surface ozone pollution in 2010 in Africa (Lelieveld et al.,. 2015). Also, increased amount of BC in the atmosphere and its ability to absorb both longwave and shortwave could contribute to an increase in local temperature that possibly will enhance the effects of climate change in the region.

Seasalt aerosol spatial distributions over African continent is presented in Fig. 1f. High Seasalt burden are seen in both the southern and northern Atlantic Oceans with the later showing highest burden ranged $2.5 \times 10^{-5}\ kgm^{-6} - 4.0 \times 10^{-5}\ kgm^{-2}$, and also, equatorial region down to low latitude Indian Sea show high concentrations though a little lower than seen in the northern Atlantic. Seasalt aerosol originates from water bodies. Therefore, this high burden seen in the oceans are expected values. Seasalt is hygroscopic in nature with the size of coarse mode aerosols such as found in Nigeria [57]. The burden of sulfate aerosol is highest in the north eastern part precisely Eritrea, Djibouti and the Gulf of Aden with values of $2.0 \times 10^{-5}\ kgm^{-2} - 2.4 \times 10^{-5}\ kgm^{-2}$ (Fig. 1g). Northern Africa and parts of west and central Africa also show considerable concentrations of sulfate aerosols. This highest concentrations is attributed to the region's prone to volcanic activity that is the main natural source of sulfate, it is also produced as a by-product of burning of fossil fuels that are adulterated with sulfur compounds. Exposure to sulfate aerosols can cause deterioration of health and environmental effects, including acid precipitation, damage to plant life and human structures among others. Furthermore, sulfate aerosols are radiatively important because of their ability to scatter shortwave radiation. Increase in the amount of sulfate aerosols in the atmosphere lessen the incoming radiation from reaching the Earth's surface, and results in surface temperature drop, thus reducing the average temperature of the local environment. In Nigeria, sulfate aerosol burden is estimated from the model to range from $7.0 \times 10^{-5}\ kgm^{-2}$ in most part of Nigeria to $10.0 \times 10^{-5}\ kgm^{-2}$ in the far north eastern part (Maiduguri).

Although, there is limited aerosol measurement stations in Nigeria, CAM-chem estimates AOD and other aerosols spatial distributions well in this region but the concentrations are uncertain. Further work is needed to improve the representation of POM and SOA as evaluated in Ref. [58]. Large uncertainties exist in the amount of global SOA distribution from observations, and the representation of these aerosols in models [59].

3.2. Comparison of AERONET and MODEL AOD

In this subsection, we focus on evaluation of the MODEL AOD (CAM-chem) against the AERONET AOD observation both at wavelength 550 nm for a period 2005–2014 at Ilorin AERONET site in Nigeria. Multi-year mean is computed for ARONET AOD, MODEL AOD and model dust for the comparison. Fig. 2 depicts temporal distribution of AOD at Nigeria's only AERONET site. On the y-axis is AOD and the number of days in a year on the x-axis.

Decade (2005 − 2014) AERONET AOD are plotted as multi-year distributions and yearly mean AOD is computed from same data and compared to the corresponding mean MODEL AOD and dust. We observed a seasonal U-shape pattern in AOD distribution with high (>0.6) AOD values falling mainly in the months of Harmattan (DJF) that is characterized as peak dry-cold season (Fig. 2).

This is the season with highest dust aerosols as a consequence of transported desert dust from the Northern Sahara coupled with biomass emissions in preparation of agriculture farming season in Nigeria. Also, in pre-monsoon (MAM) we observed a high AOD values, could be mainly from the local sources. Monsoon (JJA) and post-monsoon (SON) shows a decrease in AOD as JJA is the major wet season in Nigeria, hence, the reason for these observed decrease in AOD values in comparison to Harmattan and pre-monsoon seasons. Further, multi-year mean AERONET AOD and simulated MODEL AOD and dust show a zigzag pattern throughout the period of study. Table 1 present comparative descriptive statistical analysis between AERONET AOD and MODEL AOD and dust. We use partial correlations matrix to compute the relationships.

Decadal (2005–2014) mean AOD from the Ilorin AERONET site in Nigeria shows high value of 0.634 conditional to standard deviation = ± 0.082, and the corresponding CAM-chem simulated MODEL AOD is approximately 34% lower, and 67% lower for the simulated dust, subject to the standard deviation = ± 0.051 and ± 0.037 respectively (Table 1). Additionally, correlation coefficient shows *r* = 0.317, 0.307 and 0.812 for AERONET AOD vs. MODEL AOD, AERONET AOD vs. MODEL dust and MODEL AOD vs. MODEL
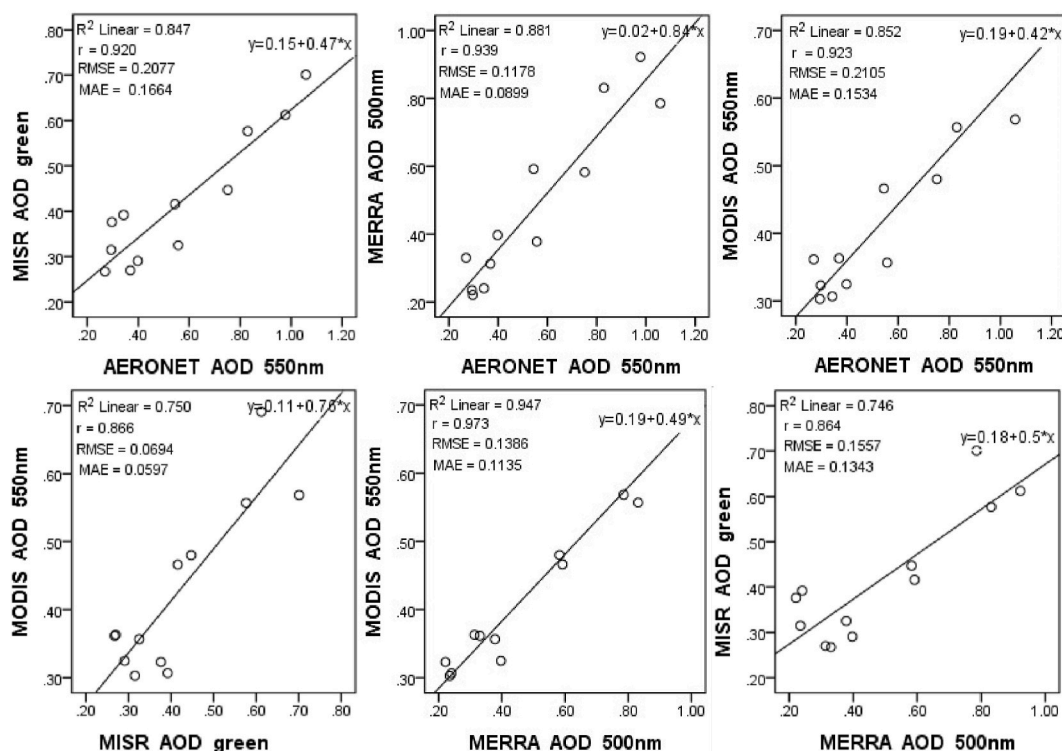
Fig. 3. Scatter plots presenting validation of (a) MISR AOD against AERONET AOD retrieved at green 558 nm and 550 nm (2005–2017), (b) MERRA-2 AOD against AERONET AOD at 500 nm and 550 nm (2005–2020), (c) MODIS AOD against AERONET AOD at 550 nm (2005–2020), (d) MODIS.

dust successively. Of course subject to RMSE = 0.229, 0.427, 0.208 and MAE = 0.215, 0.421 and 0.205 Table 1. We can deduce from the comparison that the CAM-chem simulated the AOD value with 66% accuracy in context with sunphotometer surface observation. Thus, underestimate the AOD value by 34%. The difference seen in values of AERONET AOD and MODEL AOD at Ilorin site in Nigeria could be caused by uncertainties in emissions, transport or meteorology used in the model configuration. More observations sites of aerosol properties including spatial and temporal distributions of aerosols are required for better understanding of aerosol properties in Nigeria and to identify possible reasons for underestimation of AOD in the model output.

3.3. Comparison of AOD from MODIS, MISR, MERRA-2 and AERONET

Aerosol optical depth is an important parameter in air quality as well as climate studies because it determines aerosol load in the atmosphere, we look at AOD within the visible spectrum from surface AERONET observation to validate two spectroradiometers AOD retrievals particularly MODIS AOD and MISR AOD and also employ a reanalysis model MERRA-2 AOD in order to have a comprehensive comparison at the Ilorin AERONET site in Nigeria, based on the literatures for example [60] we adopt the statistical approach as well here to evaluate the relations in AOD changes from the Four AOD datasets under study. Data period of 16-years (2005 − 2020) for AERONET, MODIS and MERRA-2 and 13-years (2005 − 2017) available data from MISR are employed.

AOD against MISR AOD at 550 nm and green 558 nm (2005–2017), MODIS AOD against MERRA2 AOD at 550 nm and 500 nm (2005–2020), and MISR AOD against MERRA-2 AOD at green 558 nm and 500 nm (2005–2017). The black line is the regression line, *r* is correlation coefficient, R-square is coefficient of determination, RMSE is root-mean-square error at 95% confidence interval and MAE is mean absolute error.

Results of regression and statistical measures between seasonal mean of AERONET AOD (x-axis) and MISR, MERRA-2 and MODIS AODs (y-axes) obtained at wavelengths 550 nm and 558 nm in the case of MISR, are presented in Fig. 3(a − c). Taking into consideration the spatial differences between surface and satellite data and other factors such as cloud reflection and meteorological differences, time series of AOD observations, obtained with MISR, MERRA-2, MODIS and AERONET conform with each other with cross-correlation between the datasets demonstrating high degree of correlation $r = 0.920$, $r = 0.939$ and $r = 0.923$ subject to RMSE = 0.2077, 0.1178 and 0.2105 and low value of MAE = 0.1684, 0.0899 and 0.1534. This high correlation was also obtained between MODIS Collection (C6 and C6.1) and AERONET and also with China Aerosol Remote Sensing Network (CARSNET) AOD measurement elsewhere in Three sites with different surfaces in Beijing as well as in Eastern Europe [61–63]. Further, determination coefficient shows high percentage of variability of the model 84.7%, 88.1% and 85.2%. We note both lowest MAE and highest percentage with MERRA-2 and AERONET AODs that is likely resulted from combination of satellite and ground retrievals as well as model data
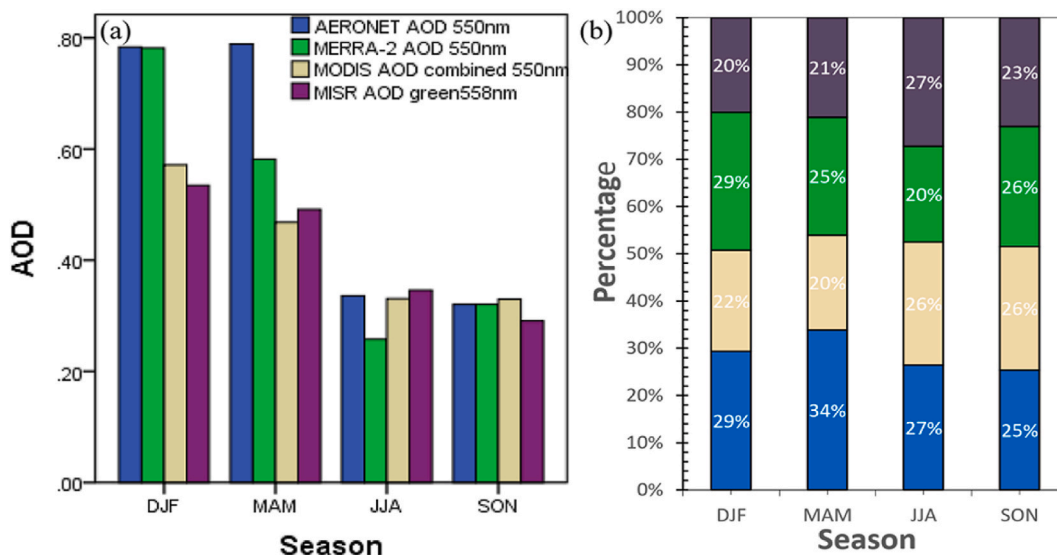
Fig. 4. Comparison of seasonal dependence of AODs from MODIS, MISR, MERRA against AERONET presented in (a) histogram and (b) stacked bar chart showing percentage of dependence in each season at Ilorin site in Nigeria.

incorporated in MERRA-2 model.

Also, cross-correlation between the two spectroradiometers show high correlation of 75% in AOD retrievals with RMSE = 0.0694 and MAE 0.0598 (Fig. 3d), this shows similarities and productivity in the two measurement methods and good representation from the two retrievals. In addition MODIS and MERRA AODs, and MISR and MERRA AODs is 94.7% and 74.6% correlated respectively.

Overall, the two spectroradiometers and MERRA-2 both show good results in this site, providing a precise representation of aerosol optical depth values under usual condition of atmospheric aerosols load, giving room for further analysis at broader frequency.

3.4. Seasonal AOD variations

AOD changes demonstrated different seasonal characteristics in the study site, signifying high share of local sources of pollution and transported desert dust aerosols from the Sahara. Sixteen (16) years seasonal mean AOD from MODIS, MERRA-2 and AERONET and 13-years seasonal mean from MISR computed from retrieves AOD over Ilorin AERONET site in Nigeria is characterized by high indices with maximum value of ~0.8 in the season that is characterized as peak of combination of local pollution source mainly from burning of biomass associated to agriculture activities and transported desert dust from the Northern Sahara that leads to Harmattan (DJF) season to the lowest value AOD = 0.28 in monsoon (JJA) season attributed to wet scavenging in the season (Fig. 4a).

Pre-monsoon (MAM) season also shows high sunphotometer AOD values in context with the two spectroradiometers and MERRA-2. The harmattan and pre-monsoon seasons present highest disparity especially in the measurements of the two spectroradiometers compared to monsoon and post-monsoon seasons AOD measurements. This could be attributed to the season's large aerosols loading and are characterized by hazy and smoky atmosphere that reduce the visibility coupled with effect of cloud that subsequently hinder the near Earth view of the satellites. This is most likely reason for the large disparity observed between MODIS and MISR AODs against AERONET AOD in the two seasons in addition to algorithm explanation given by Ref. [60]. On the other hand, Fig. 4b provides in stacked bar chart clearly the seasonal percentage contribution of each observation compared to AERONET observation totaling hundred percent. Using AERONET AOD observation as a reference point, MERRA-2 simulated AOD over Ilorin site in Nigeria obviously shows good agreement of 29% and 25% for harmattan and pre-monsoon seasons respectively, when compared to the percentage contribution from MODIS (22%/20%) and MISR(20%/21%) in same seasons. These two season have not present good correlations between AERONET AOD and MODIS/MISR AODs at this site. However, MODIS/MISR AODs shows strong conformity with AERONET 27% and 25% in monsoon and post-monsoon seasons respectively (Fig. 4b). Overall, monsoon and post-monsoon seasons show better agreement in AOD observations with sunphotometer than harmattan and pre-monsoon season's results. This shows generally that there is seasonal fluctuations and probable the strong influence of transported Saharan dust (one of the main driver of pollutants in West Africa) in the harmattan and pre-monsoon seasons is not well captured in satellite retrievals in this site.

Table 2 depicts the annual and seasonal mean AOD for all the four retrievals at the site. High and low annual mean AOD values were observed from different measurements employed. In the seasonal mean, high and low values are observed across the seasons with distinct high mean AOD values prominent in harmattan and pre-monsoon seasons in the AERONET, MERRA and MODIS/MISR though slightly lower in estimation against AERONET/MERRA in pre-monsoon seasons, and lowest values in monsoon and post-monsoon seasons and MISR showing a slight underestimation against MODIS in post-monsoon season. This high mean AOD values are due to the seasons predominance of desert dust aerosols with high mean values AOD (± standard deviation) in harmattan 0.784 ± 0.220, 0.782 ± 0.113, 0.571 ± 0.171 and in pre-monsoon 0.789 ± 0.254, 0.582 ± 0.106, 0.468 ± 0.204 for AERONET, MERRA and MODIS

Table 2

Annual and seasonal means and standard deviations of AERONET AOD (550 nm), MERRA AOD (500 nm), MODIS AOD (550 nm) and MISR AOD (green 558 nm) during 2005 – 2020.

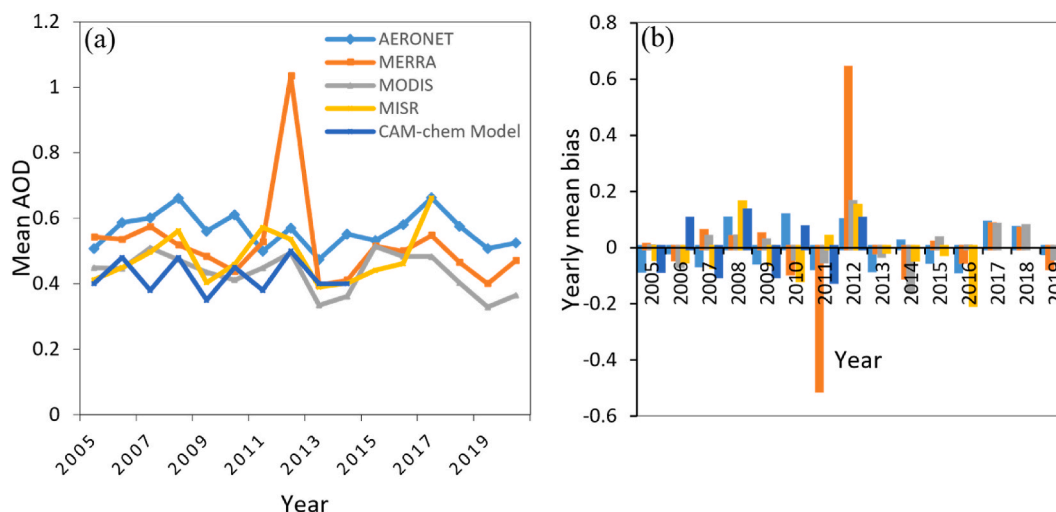|	AERONET					MERRA					MODIS					MISR				
	Annual mean	Harmattan	Pre-monsoon	Monsoon	Post-monsoon	Annual mean	Harmattan	Pre-monsoon	Monsoon	Post-monsoon	Annual mean	Harmattan	Pre-monsoon	Monsoon	Post-monsoon	Annual mean	Harmattan	Pre-monsoon	Monsoon	Post-monsoon
Ilorin	0.557 ± 0.281	0.784 ± 0.220	0.789 ± 0.254	0.336 ± 0.036	0.321 ± 0.068	0.487 ± 0.249	0.782 ± 0.113	0.582 ± 0.106	0.258 ± 0.029	0.321 ± 0.029	0.426 ± 0.126	0.571 ± 0.171	0.468 ± 0.204	0.331 ± 0.048	0.329 ± 0.081	0.416 ± 0.143	0.535 ± 0.105	0.491 ± 0.192	0.346 ± 0.066	0.291 ± 0.024

Fig. 5. The interannual variations of the: (a) yearly mean MERRA, MODIS, MISR, CAM-chem model and AERONET AODs and (b) yearly mean bias, at Ilorin site in Nigeria from 2002 to 2020.

accordingly. And lowest mean AOD values in monsoon and post-monsoon seasons of.

0.336 ± 0.036, 0.321 ± 0.068, 0.258 ± 0.029, 0.321 ± 0.029, 0.331 ± 0.048, 0.329 ± 0.081 and 0.346 ± 0.066, 0.291 ± 0.024 for AERONET, MERRA, MODIS and MISR successively. We could observe that the AOD values fluctuations across the seasons are well pronounce in AERONET measurements and MERRA modeling but lightly shown with MODIS/MISR retrievals. This could be attributed to coarser feature of satellites retrievals. Overall, the annual and seasonal mean AOD values obtained across the seasons with all the four datasets show seasonal dependence.

3.5. Inter-annual variability of AOD and anomaly

It is apparent from Fig. (5) (a) that there is a year-to-year variability in all the five computed yearly mean AOD datasets and in general, MODIS registered lowest AOD value of 0.3286 in 2019 and AERONET presents trend with highest AOD yearly mean value almost throughout the years of study with marked highest value of 0.6625 in 2017, excluding an exceptional trend presented by MERRA with highest yearly mean value of 1.0335 in 2012.

This large value registered by MERRA may likely resulted from an uncertainty in MERRA modeling. A gradual decline in aerosol concentration to -0.0067 (from 0.5072 in 2005 to 0.5517 in 2014), -0.0031 (from 0.4485 in 2005 to 0.3645 in 2014), -0.0045 (from 0.4119 in 2005 to 0.4014) on decadal levels were observed for AERONET/MODIS/MISR successively, and a gradual increase noted with MERRA 0.0039 (from 0.5429 in 2005 to 0.5144 in 2014). Further, CAM-chem model AOD shows its lowest estimated value in 2009 with a slight difference of 0.0214 when compared to overall minimum AOD from MODIS, and 0.0533 from MISR 2019 measurement. Also, CAM-chem model estimated AOD yearly mean = 0.5 is registered as maximum value in 2012 which corresponds to 0.57(AERONET), 0.53(MISR) and 0.49(MODIS) Fig. (5) (a).

The interannual variability of AOD values over Ilorin AERONET site in Nigeria does not show a consistent steady nor gradual decrease in AOD values in the years under study, this could be due to limited stringent measures to control anthropogenic emissions in the country.

Figure (5) (b)) demonstrates the AOD yearly. The anomalies of the sunphotometer and the two spectroradiometers are confined within ± 0.2 for all the years of study but that of MERRA in year 2011/2012 presents very abnormal scenario, a decreased values of -0.5064 (in 2011) and increased of 0.6373 (in 2012) in MERRA, and an increased value of 0.4 (in 2014) in CAM-chem models in comparison with other years even within MERRA model.

There is almost a steady anomaly decrease in AOD from 2005 to 2007 and 2013 to 2016/2019 ranged between -0.081 to -0.014 (in AERONET), -0.506 to -0.014 (in MERRA, large uncertainty included), -0.153 to -0.027 (in MODIS), -0.201 to -0.012 (in MISR) and -0.12 to -0.08 (in CAM-chem) with maximum and minimum uncertainty presented by MISR and MERRA in 2013 and 2011 respectively.

On the other side, an increase in AOD anomaly in major parts of dataset in particularly in 2008, 2009(MERRA/MISR, 2009 (AERONET) and 2012. A continues decrease is observed from 2013 to 2016 with slight increase in 2015, and then a sudden drop in AOD in the anomaly of 2019 and 2020, which is attributed to Covid-19 pandemic lockdown restriction measures that caused a significant halt in anthropogenic emissions from energy/industrial and transport sectors in Nigeria and the world over. AOD positive anomaly shows maximum and minimum values of ~0.637 in 2012 and ~0.001 in 2016 from MERRA and MODIS respectively. Overall, there is decrease and increase fluctuations between the years of study among the Aura MODIS/MISR satellites and also MERRA and CAM-chem models and AERONET surface observation. This disparity is attributed to the differences in satellite instrumentation, calibration as well as algorithm in aerosol retrievals [44]; Zhang and Reid, 2010; [64].

Table 3

Annual mean Partial (Spearman) Correlations of AOD from AERONET, MERRA/MODIS/MISR and CAM-chem.

Control Variables			AERONET AOD 550 nm	MERRA AOD 500 nm	MODIS AOD 550 green	MISR AOD 558 nm nm	CAM-chem AOD 550 nm
Year	AERONET AOD 550 nm	Correlation	1.000				
		Significance (2tailed)	.				
		df	0				
	MERRA AOD 500 nm	Correlation	.149	1.000			
		Significance (2tailed)	.702	.			
		df	7	0			
	MODIS AOD 550 nm	Correlation	.423	.794	1.000		
		Significance (2tailed)	.257	.011	.		
		df	7	7	0		
	MISR AOD green 558 nm	Correlation	.402	.491	.789	1.000	
		Significance (2tailed)	.284	.179	.011	.	
		df	7	7	7	0	
	CAM-chem AOD 550 nm	Correlation	.529	.517	.287	.401	1.000
		Significance (2tailed)	.143	.154	.454	.285	.
		df	7	7	7	7	0

Table 4

Descriptive statistic of the mean annual AOD measurements from AERONET, MERRA/MODIS/MISR and CAM-chem.

	N	Range	Minimum	Maximum	Sum	Mean		Std. Deviation	Variance
	Statistic	Statistic	Statistic	Statistic	Statistic	Statistic	Std. Error	Statistic	Statistic
AERONET AOD 550 nm	16	.19	.47	.66	9.01	.5629	.01374	.05494	.003
MERRA AOD 500 nm	16	.64	.40	1.03	8.36	.5223	.03674	.14695	.022
MODIS AOD 550 nm	16	.19	.33	.51	6.94	.4337	.01516	.06065	.004
MISR AOD 558 nm	13	.27	.39	.66	6.24	.4804	.02261	.08153	.007
CAM-chem AOD 550 nm	10	.15	.35	.50	4.22	.4220	.01625	.05138	.003
Valid N (listwise)	10								

We applied Spearman partial correlations to compare the interannual variability statistically. The annual mean of AOD from MERRA/MODIS/MISR and CAM-chem against AERONET is computed and presented in Table 3. Although, we all have positive relationships which indicate an upward slope, but the correlation coefficient between AERONET/MODIS, AERONET/MISR and AERONET/MERRA are less than average (<0.5) with AERONET/MERRA showing the least relation in the assessment (2004–2020) AOD observations over Ilorin AERONET site in Nigeria. AERONET/CAM-chem shows correlation coefficient value ($r = 0.529$), which is classified as fairly good correlation. Overall, MERRA/MODIS and MODIS/MISR shows strong and significant positive relationship with p-value of 0.011 and 0.011 respectively. Low variance and standard deviation and also standard error are observed in all the AOD measurements under study except a little higher in MERRA AOD modeling (Table 4).

4. Conclusion

Desert dust and black carbon as estimated in CAM-chem are the largest contributor to air pollution in the African continent. Black carbon shows its largest burden in Nigeria attributed to gas flares and biomass emissions. The high dust aerosol burden seen over Nigeria from the model coincide with the results obtained in Ref. [37] that found high percentage (76%) of coarse dust aerosol as dominance, established based on particle size and volume size distribution at same AERONET Ilorin site. CAM-chem estimates AOD and other aerosols spatial distributions well in this region but the concentrations are uncertain. Both primary organic matter and secondary organic aerosol burdens show substantial concentration but primary organic matter is more disperse over Africa compared to secondary organic aerosol that shows twice larger burden. North African region show relatively low primary organic matter and secondary organic aerosol burden. The burden of sulfate aerosol is highest in the north eastern part precisely Eritrea, Djibouti and the Gulf of Aden. The harmattan and pre-monsoon seasons present highest disparity especially in the measurements of the two spectroradiometers compared to monsoon and post-monsoon seasons AOD measurements. The annual and seasonal mean AOD values obtained across the seasons with all the four datasets show seasonal dependence. Overall, monsoon and post-monsoon seasons show better agreement in AOD observations with sunphotometer than harmattan and pre-monsoon season's results. Probable the strong influence of transported Saharan dust (one of the main driver of pollutants in West Africa) in the harmattan and pre-monsoon seasons is not well captured by satellites AOD retrievals in this site. A year-to-year variability in all the five computed yearly mean AOD datasets are observed and in general, MODIS registered lowest value in 2019 and AERONET presents highest value of 0.6625 in 2017, excluding an exceptional trend presented by MERRA with highest yearly mean value in 2012. The computed annual mean of AOD from MERRA/MODIS/MISR and CAM-chem against AERONET have all shown positive relationships which indicate an upward slope, but the correlation coefficient between AERONET/MODIS, AERONET/MISR and AERONET/MERRA are less than average (<0.5) with AERONET/MERRA showing the least relation in the assessment period (2004–2020) of AOD observations. AERONET/CAM-chem

shows correlation coefficient value ($r = 0.529$), which is classified as fairly good correlation. Overall, MERRA/MODIS and MODIS/MISR shows strong and significant positive relationship. Low variance and standard deviation and also standard error are observed in all the different AOD measurement under study except a little higher in MERRA AOD modeling.

Author contribution statement

Najib Yusuf conceived and designed the experiments, perform the experiment, analyzed and interpreted the data, wrote the paper. Rabia Said S. conceived and designed the experiments, wrote the paper.

Data availability statement

Data associated with this study has been deposited at AERONET WEB PAGE, NASA EARTH DATA (GIOVANNI V 4.38) AND NCAR DATA REPOSITORY.

Declaration of competing interest

The authors declare that they have no known competing financial interests or personal relationships that could have appeared to influence the work reported in this paper.

Acknowledgement

References

[1] J. Lelieveld, J.S. Evans, M. Fnais, D. Giannadaki, A. Pozzer, The contribution of outdoor air pollution sources to premature mortality on a global scale, Nature 525 (2015) 367–371. https://doi.org/10.1038/nature15371.

[2] E.P. Petkova, D.W. Jack, N.H. Volavka-Close, P.L. Kinney, Particulate matter pollution in African cities, Air Quality, Atmosphere & Health 6 (2013) 603–614, https://doi.org/10.1007/s11869013-0199-6.

[3] A.K. Amegah, S. Agyei-Mensah, Urban air pollution in sub-saharan Africa: time for action, Environmental Pollution 220 (2017) 738–743, https://doi.org/10.1016/j.envpol.2016.09.042. Part A).

[4] S.E. Bauer, U. Im, K. Mezuman, C.Y. Gao, Desert dust, industrialization, and agricultural fires: health impacts of outdoor air pollution in Africa, J. Geophys. Res. Atmos. 124 (2019) 4104–4120, https://doi.org/10.1029/2018JD029336.

[5] T.F. Eck, B. Holben, A. Sinyuk, R. Pinker, P. Goloub, H. Chen, et al., Climatological Aspects of the Optical Properties of Fine/coarse Mode Aerosol Mixtures, vol. 115, 2010, D19205, https://doi.org/10.1029/2010JD014002.

[6] D.M. Giles, B.N. Holben, T.F. Eck, A. Sinyuk, A. Smirnov, I. Slutsker, et al., An analysis of AERONET aerosol absorption properties and classifications representative of aerosol source regions, J. Geophys. Res. 117 (2012), D17203, https://doi.org/10.1029/2012JD018127.

[7] M.O. Andreae, D. Rosenfeld, Aerosol-cloud-precipitation interactions, Part 1, Earth Sci. Rev. 89 (2008) 13–41, https://doi.org/10.1016/j.earscirev.2008.03.001.

[8] C.H. Mari, E.R. Claire, S.L. Katherine, E.W. Jason, Atmospheric composition of west Africa: highlights from the AMMA international program, Atmos. Sci. Lett. 12 (2010) 3–8.

[9] B. Marticorena, J. Haywood, H. Coe, P. Formenti, C. Liousse, M. Mallet, J. Pelon, Tropospheric aerosols over West Africa: highlights from the AMMA international program, Atmosph. Sci. Lett. 12 (2011) 19–23. https://doi.org/10.1002/asl.322.

[10] C. Liousse, J.E. Penner, C. Chuang, J.J. Walton, H. Eddleman, H. Cachier, A global three dimensional model study of carbonaceous aerosols, J. Geophys. Res. 101 (2010) 19411–19432.

[11] F. Malavelle, V. Pont, M. Mallet, F. Solmon, B. Johnson, J. Leon, C. Liousse, Simulation of aerosol radiative effects over West Africa during DABEX and AMMA SOP0, J. Geophys. Res. 116 (2011) D18.

[12] P. Knippertz, A.H. Fink, A. Deroubaix, E. Morris, F. Tocquer, M.J. Evans, et al., A meteorological and chemical overview of the field campaign in West Africa in June–July 2016, Atmos. Chem. Phys. 17 (17) (2017) 10893–10918, https://doi.org/10.5194/acp-17-10893-2017.

[13] E.A. Marais, C. Wiedinmyer, 2013, Environ. Sci. Technol. (50) (2016) 10739–10745.

[14] C. Liousse, E. Assamoi, P. Criqui, C. Granier, R. Rosset, Explosive growth in african combustion emissions from 2005 to 2030, Environ. Res. Lett. 9 (2014), 035003, https://doi.org/10.1088/1748-9326/9/3/035003, 10.

[15] L. Menut, B. Bessagnet, D. Khvorostyanov, M. Beekmann, N. Blond, A. Colette, et al., Chimere 2013: a model for regional atmospheric composition modelling, Geosci. Model Dev. (GMD) 6 (2013) 981–1028, https://doi.org/10.5194/gmd-6-981-2013.

[16] C. Fountoukis, A.G. Megaritis, K. Skyllakou, P.E. Charalampidis, H.A.D.C. van der Gon, M. Crippa, et al., Simulating the formation of carbonaceous aerosol in a European Megacity (Paris) during the MEGAPOLI summer and winter campaigns, Atmos. Chem. Phys. 26 (2016) 3727–3741.

[17] Z.A. Chafe, M. Bauer, Z. Klimont, R. Van Dingenen, S. Mehta, S. Rao, et al., Household cooking with solid fuels contributes to ambient PM2.5 air pollution and the burden of disease Environ, Health Perspect. 122 (2014) 1314–1320.

[18] K.R. Smith, et al., Millions Dead: how do we know and what does it mean? Methods used in the Comparative Risk Assessment of household air pollution, Annu. Rev. Publ. Health 35 (2014) 185–206.

[19] S.C. Anenberg, L.W. Horowitz, D.Q. Tong, J.J. West, An estimate of the global burden of anthropogenic ozone and fine particulate matter on premature human mortality using atmospheric modeling, Environ. Health Perspect. 118 (2010) 1189–1195.

[20] S.S. Lim, et al., A comparative risk assessment of burden of disease and injury attributable to 67 risk factors and risk factor clusters in 21 regions, 1990–2010, a systematic analysis for the global burden of disease study 2010, Lancet 380 (2012) 2224–2260.

[21] S.C. Anenberg, K. Balakrishnan, J. Jetter, O. Masera, S. Mehta, J. Moss, V. Ramanathan, Cleaner cooking solutions to achieve health, climate, and economic co-benefits, Environ. Sci. Technol. 47 (2013) 3944–3952.

[22] F. Lacey, D. Henze, Global climate impacts of country level primary carbonaceous aerosol from solid-fuel cookstove emissions, Environ. Res. Lett. 10 (2015), 114003.

[23] M. Filonchyk, H. Yan, Z. Zhang, Analysis of spatial and temporal variability of aerosol optical depth over China using MODIS combined Dark Target and Deep Blue product, Theor. Appl. Climatol. (2018) 1–18, https://doi.org/10.1007/s00704-018-2737-5, 2018.

[24] H. Che, et al., Ground-based aerosol climatology of China: aerosol optical depths from the China Aerosol Remote Sensing Network (CARSNET) 2002–2013, Atmos. Chem. Phys. 15 (13) (2015) 7619–7652.

[25] M.M. Rienecker, Coauthors, Atmospheric Reanalyses: Recent Progress and Prospects for the Future, vol. 29, NASA GSFC, 2011, p. 35. NASA/TM-2011-104606.

[26] J.W. Hurrell, M.M. Holland, P.R. Gent, S. Ghan, J.E. Kay, P.J. Kushner, et al., The Community Earth System Model: a framework for collaborative research, Bull. Am. Meteorol. Soc. 94 (2013) 1339–1360, https://doi.org/10.1175/BAMS-D-12-00121.1.

[27] P.A. Bogenschutz, A. Gettelman, C. Hannay, V.E. Larson, R.B. Neale, C. Craig, C.-C. Chen, The path to CAM6: coupled simulations with CAM5.4 and CAM5.5, Geosci. Model Dev. 11 (2018) 235–255. https://doi.org/10.5194/gmd-11-235-2018.

[28] S. Tilmes, J.F. Lamarque, L.K. Emmons, D.E. Kinnison, N. Blake, Representation of the Community Earth System Model (CESM1) CAM4-Chem within the Chemistry-Climate Model Initiative (CCMI), 2016.

[29] L.K. Emmons, S. Walters, P.G. Hess, J.-F. Lamarque, G.G. Pfister, D. Fillmore, C. Granier, A. Guenther, D. Kinnison, T. Laepple, et al., Description and evaluation of the model for ozone and related chemical tracers, version 4 (MOZART-4), Geosci. Model. Dev. 2010 3 (2010) 43–67.

[30] X. Liu, et al., Toward a minimal representation of aerosols in climate models: description and evaluation in the Community Atmosphere Model CAM5, Geosci. Mod. Dev. 5 (2012) 709–739, https://doi.org/10.5194/gmd-5-709.

[31] X. Liu, H. Wang, S. Tilmes, B. Singh, R.C. Easter, S.J. Ghan, P.J. Rasch, Description and evaluation of a new four model version of the modal aerosol module (MAM4) within version 5.3 of the community atmosphere model, Geosc. Mod. Dev. 9 (2016) 505–522, https://doi.org/10.5194/gmd-9-505.

[32] M.J. Mills, et al., Global volcanic aerosol properties derived from emissions, 1990–2014, using CESM1 (WACCM), J. Geophys. Res. Atmos. 121 (2016) 2332–2348, https://doi.org/10.1002/2015JD024290.

[33] A. Hodzic, P.S. Kasibhatla, D.S. Jo, C.D. Cappa, J.L. Jimenez, S. Madronich, et al., Rethinking the global secondary organic aerosol (SOA) budget: stronger production, faster removal, shorter lifetime, Atmos. Chem. Phys. 16 (2016) 7917–7941, https://doi.org/10.5194/acp.

[34] S. Tilmes, A. Hodzic, L.K. Emmons, M.J. Mills, A. Gettelman, D.E. Kinnison, et al., Climate forcing and trends of organic aerosols in the community earth system model (CESM2), J. Adv. Model. Earth Syst. 11 (2019) 4323–4351, https://doi.org/10.1029/2019MS001827.

[35] B. Holben, T. Eck, I. Slutsker, D. Tanre, J. Buis, A. Setzer, et al., AERONET: a federated instrument network and data archive for aerosol characterization, Remote Sens. Environ. 66 (1) (1998) 1–16.

[36] A. Smirnov, T.F. Eck, O. Dubovik, I. Slutsker, Cloud screening and quality control algorithms for the AERONET data base, Remote Sens. Environ. 73 (2000) 337–373 349.

[37] N. Yusuf, S.S. Rabia, S. Tilmes, E. Gbobaniyi, Multi-year analysis of aerosol optical properties at various timescales using AERONET data in tropical West Africa, J. Aerosol Sci. 151 (2021), 105625, https://doi.org/10.1016/j.jaerosci.2020.105625. ISSN 0021-8502.

[38] O. Dubovik, A. Smirnov, B. Holben, M. King, Y.J. Kaufman, T.F. Eck, et al., Accuracy assessments of aerosol optical properties retrieved from Aerosol Robotic Network (AERONET) Sun and sky radiance measurements, J. Geophys. Res. 105 (D8) (2000) 9791–9806, https://doi.org/10.1029/2000JD900040.

[39] O. Dubovik, B. Holben, T.F. Eck, A. Smirnov, Y.J. Kaufman, M.D. King, et al., Variability of absorption and optical properties of key aerosol types observed in worldwide locations, J. Atmos. Sci. 59 (3) (2002) 590–608.

[40] Jean-François Léon, Aristide Barthélémy Akpo, Mouhamadou Bedou, Julien Djossou, Marleine Bodjrenou, Véronique Yoboué, Cathy Liousse, PM2:5 surface concentrations in southern West African urban areas based on sun photometer and satellite observations, Atmos. Chem. Phys. 21 (2021) 1815–1834, https://doi.org/10.5194/acp-21-1815-2021.

[41] C. Justice, J. Townshend, Special issue on the moderate resolution imaging spectroradiometer (MODIS): a new generation of land surface monitoring, Remote Sens. Environ. 83 (2002) 1–2, https://doi.org/10.1016/S0034-4257(02)00083-4.

[42] M.J.M. Penning de Vries, S. Beirle, C. Hörmann, J.W. Kaiser, P.L. Stammes, G. Tilstra, O.N.E. Tuinder, T. Wagner, A global aerosol classification algorithm incorporating multiple satellite data sets of aerosol and trace gas abundances, Atmos. Chem. Phys. 15 (2015) 10597–10618, https://doi.org/10.5194/acp-15-10597-2015.

[43] N.C. Hsu, et al., Enhanced deep blue aerosol retrieval algorithm: the second generation, J. Geophys. Res. Atmos. 118 (2013) 9296–9315.

[44] H. Levy, et al., The roles of aerosol direct and indirect effects in past and future climate change, J. Geophys. Res. Atmos. 118 (10) (2013) 4521–4532.

[45] J. Wei, Y. Peng, J. Guo, L. Sun, Performance of MODIS collection 6.1 level 3 aerosol products in spatial-temporal variations over land, Atmos. Environ. 206 (2019) 30–44, https://doi.org/10.1016/j.atmosenv.2019.03.001.

[46] J.A. Ruiz-Arias, J. Dudhia, C.A. Gueymard, D. Pozo-Vázquez, Assessment of the Level-3 MODIS daily aerosoloptical depth in the context of surface solar radiation and numerical weather modeling, Atmos. Chem. Phys. 13 (2013) 675–692, https://doi.org/10.5194/acp13-675-2013.

[47] A.M. Sayer, L.A. Munchak, N.C. Hsu, R.C. Levy, C. Bettenhausen, M.-J. Jeong, MODIS collection 6 aerosol products: comparison between aqua's e-deep blue, dark target, and "merged" data sets, and usage recommendations, J. Geophys. Res. Atmos. 119 (2014) 13965–13989, https://doi.org/10.1002/2014JD022453, 2014.

[48] C. Ichoku, D.A. Chu, S. Mattoo, Y.J. Kaufman, L.A. Remer, D. Tanré, I. Slutsker, B.N. Holben, A spatio-temporal approach for global validation and analysis of MODIS aerosol products, Geophys. Res. Lett. 29 (2002) MOD1–1, https://doi.org/10.1029/2001GL013206.

[49] F. Rubel, M. Kottek, Comments on: the thermal zones of the earth' by wladimir köppen (1884), Meteorologische Zeitschrift. 20 (3): Bibcode: 2011MetZe.20.361R (2011), https://doi.org/10.1127/0941-2948/2011/0258.

[50] Köppen Wladimir, Die Wärmezonen der Erde, nach der Dauer der heissen, gemässigten und kalten Zeit und nach der Wirkung der Wärme auf die organische Welt betrachtet" [The thermal zones of the earth according to the duration of hot, moderate and cold periods and to the impact of heat on the organic world)], Translated by Volken, E.; Brönnimann, S, Meteorol. Z. 20 (3) (1884) 351–360, 2011.

[51] J.D. David. MISR observing concept, JPL. Cal. Tech., 2005. Workshop May 22.

[52] R.A. Kahn, et al., Multiangle Imaging SpectroRadiometer global aerosol product assessment by comparison with the Aerosol Robotic, Network. J. Geophys. Res. Atmos. 115 (2010) D23209.

[53] W. McCarty, L. Coy, R. Gelaro, A. Huang, D. Merkova, E.B. Smith, M. Sienkiewicz, K. Wargan, MERRA-2input Observations: Summary and Assessment. NASA TM-2016- 104606, vol. 46, NASA Global Modeling and Assimilation Office, 2016, p. 64 [Available online at: https://gmao.gsfc.nasa.gov/reanalysis/MERRA-2/docs/.

[54] W.-S. Wu, R. Purser, D. Parrish, Three-dimensional variational analysis with spatially inhomogeneous covariances, Mon. Wea. Rev. 130 (2002) 2905–2916, 10.1175/15200493(2002)130,2905:TDVAWS.2.0.CO;2.

[55] D.T. Kleist, D.F. Parrish, J.C. Derber, R. Treadon, W.-S. Wu, S. Lord, Introduction of the GSI into the NCEP global data assimilation system, Weather Forecast. 24 (2009) 1691–1705, https://doi.org/10.1175/2009WAF2222201.1.

[56] D. Bhattu, Primary organic aerosols, in: N. Sharma, A. Agarwal, P. Eastwood, T. Gupta, A. Singh (Eds.), Air Pollution and Control. *Energy, Environment, and Sustainability*, Springer, Singapore, 2018, https://doi.org/10.1007/978-981-10-7185-0_7.

[57] A. McComiskey, Aerosols and Radiation - NOAA Earth System Research Laboratory, 2017. https://en.wikipedia.org/wiki/Sea_salt_aerosol#cite_note-1/. (Accessed 7 May 2018).

[58] K. Tsigaridis, et al., The AeroCom evaluation and intercomparison of organic aerosol in global models, Atmos. Chem. Phys. 14 (2014) 10845–10895, https://doi.org/10.5194/acp-14-10845-2014.

[59] S. Tilmes, J.-F. Lamarque, L.K. Emmons, D.E. Kinnison, P.-L. Ma, X. Liu, S. Ghan, C. Bardeen, S. Arnold, M. Deeter, F. Vitt, T. Ryerson, J.W. Elkins, F. Moore, J. R. Spackman, M. Val Martin, Description and evaluation of tropospheric chemistry and aerosols in the community earth system model (CESM1.2), Geosci. Model Dev. (GMD) 8 (2015) 1395–1426, https://doi.org/10.5194/gmd-8-1395-2015.

[60] M. Filonchyk, H. Yan, Z. Zhang, et al., Combined use of satellite and surface observations to study aerosol optical depth in different regions of China, Sci. Rep. 9 (2019) 6174, https://doi.org/10.1038/s41598-019-42466-6.

[61] Muhammad Bilal, Majid Nazeer, Janet Nichol, Zhongfeng Qiu, Lunche Wang, Max P. Bleiweiss, Xiaojing Shen, James R. Campbell, Simone Lolli, Evaluation of terra-MODIS C6 and C6.1 aerosol products against beijing, XiangHe, and xinglong AERONET sites in China during 2004-2014, Rem. Sens. 11 (5) (2019) 486, https://doi.org/10.3390/rs11050486.

[62] Che, et al., Long-term validation of MODIS C6 and C6.1 Dark Target aerosol products over China using CARSNET and AERONET, Chemosphere 236 (2019), 124268, https://doi.org/10.1016/j.chemosphere.2019.06.238. ISSN 0045-6535.

[63] M. Filonchyk, V. Hurynovich, Validation of MODIS aerosol products with AERONET measurements of different land cover types in areas over eastern Europe and China, J geovis spat anal 4 (2020) 10, https://doi.org/10.1007/s41651-020-00052-9, 2020.

[64] D.G. Streets, et al., Aerosol trends over China, 1980–2000, Atmos. Res. 88 (2) (2008) 174–182.